Research Paper

Role of Nrf2 and protective effects of Metformin against tobacco smoke-induced cerebrovascular toxicity

CrossMark

Shikha Prasad[a], Ravi K. Sajja[a], Mohammad Abul Kaisar[a], Jee Hyun Park[a], Heidi Villalba[a], Taylor Liles[a], Thomas Abbruscato[a,b], Luca Cucullo[a,b,*]

[a] Department of Pharmaceutical Sciences, School of Pharmacy, Texas Tech University Health Sciences Center, 1300 S. Coulter Street, Amarillo, TX 79106, USA
[b] Center for Blood Brain Barrier Research, Texas Tech University Health Sciences Center, Amarillo, TX 79106, USA

A B S T R A C T

Cigarette smoking (**CS**) is associated with vascular endothelial dysfunction in a causative way primarily related to the TS content of reactive oxygen species (**ROS**), nicotine, and inflammation. TS promotes glucose intolerance and increases the risk of developing type-2 diabetes mellitus (**2DM**) with which it shares other pathogenic traits including the high risk of cerebrovascular and neurological disorders like stroke *via* ROS generation, inflammation, and blood-brain barrier (**BBB**) impairment. Herein we provide evidence of the role played by nuclear factor erythroid 2-related factor (**Nrf2**) in CS-induced cerebrobvascular/BBB impairments and how these cerebrovascular harmful effects can be circumvented by the use of metformin (**MF**; a widely prescribed, firstline anti-diabetic drug) treatment. Our data in fact revealed that MF activates counteractive mechanisms primarily associated with the Nrf2 pathway which drastically reduce CS toxicity at the cerebrovascular level. These include the suppression of tight junction (**TJ**) protein downregulation and loss of BBB integrity induced by CS, reduction of inflammation and oxidative stress, renormalization of the expression levels of the major BBB glucose transporter Glut-1 and that of the anticoagulant factor thrombomodulin. Further, we provide additional insights on the controversial interplay between Nrf2 and AMPK.

1. Introduction

Globally, tobacco use causes approximately 6 million deaths per year, and predictions report that with current trends of tobacco use, more than 8 million deaths are expected annually by 2030. Cigarette smoking is accountable for more than 480,000 deaths each year in United States (US) and is the leading cause of preventable death in the US. What is further of concern is that 41,000 deaths out of 480,000 deaths results from secondhand smoke exposure. Nearly 50% of chronic smokers die prematurely as a result of the adverse effects of their tobacco addiction. For every individual who dies due to smoking, at least 30 people are affected and live with a severe smoking-related illness [1–3]. Smokers are 2–4 times more likely to suffer from

coronary heart disease and stroke [4] and around 25 times more likely to suffer from lung cancer. The risk of developing diabetes is 30–40% higher for smokers in comparison to nonsmokers, which further increases with the number of cigarettes smoked [2,5]. Besides these major illnesses, smoking has also been associated with the onset of rheumatoid arthritis, pneumonia, asthma, blindness, hardening of the arteries, reduced fertility and enhanced risk of infections [2,3,5,6]. From a cerebrovascular and neurological perspective, tobacco smoking (**TS**) is associated with vascular endothelial dysfunction [7–9] in a causative and dose dependent way [10] primarily related to the TS content of reactive oxygen species (**ROS**) [8,11], nicotine [12–17], and smoking-induced inflammation [18]. As such TS is also a major prodromal factor for numerous central nervous system (CNS) disorders

including Alzheimer's, depression, cognitive impairment, stroke, and vascular dementia. TS promotes glucose intolerance and increases the risk of developing type-2 diabetes mellitus (**2DM**) [19,20] with which it shares other pathogenic traits *via* ROS generation, inflammation, and blood-brain barrier (**BBB**) impairment [21–23]. It also impairs cerebrovascular development in fetus during pregnancy [5].

Even though the Food and Nutrition Board of the National Academy of Sciences recommends a higher dietary allowance (**RDA**) of vitamin C for smokers (more than 200 mg/day as compared to 90 mg/day for non-smokers), the benefits of prophylactic antioxidant use in smokers remains controversial [24,25]. Considering this premise, it is evident that studies are needed to explore biologic mechanisms by which exposure to tobacco smoke compromises health, identify biomarkers of injury, and detect smokers at early stages of disease development and find clinical drugs with prophylactic/therapeutic benefits against smoke exposure effects.

From this perspective, recent findings from our group [26] support an additive release pattern of angiogenic and inflammatory factors (besides activation of common anti-oxidant mechanisms) by BBB endothelial cells in response to hyperglycemia (**HG**) with concomitant exposure to cigarette smoke extracts (**CSE**), thus suggesting the involvement of common pathogenic modulators of BBB impairment. To this end, metformin (**MF**; a widely prescribed, firstline anti-diabetic drug) treatment before and after stroke injury has been shown to reduces stress and inhibits inflammatory responses [27,28]. Herein we provide novel *in vitro* and *in vivo* data demonstrating how MF activates counteractive mechanisms which drastically reduce TS toxicity at the cerebrovascular level. These beneficial effects are mediated by MF's activation of nuclear factor erythroid 2-related factor (**Nrf2**) [27]. These novel findings support and build on previous research from our group demonstrating that Nrf2 plays a functional role in preserving BBB integrity [29] and that alterations of gene transcription/translation related to the Nrf2-ARE pathways were among the most predominant in human BBB microvascular endothelial cells exposed to TS [30].

2. Methods

2.1. Materials and reagents

Sterile culture wares were purchased from Fisher Scientific (Pittsburgh, PA, USA), reagents and chemicals were purchased from Sigma-Aldrich (St. Louis, MO, USA) or Bio-rad laboratories (Hercules, CA, USA). Gel electrophoresis was carried out by using Mini-Protean® TGXTM gels 4–15% (#456−1084) from Bio-rad laboratories (Hercules, CA, USA). Dextran-Cascade Blue® (10,000 MW; #D-1976) was obtained from life technologies (Grand Island, NY, USA), while Fluorescein isothiocyanate (FITC)-dextran (3000–5000 MW; #FD4) and Rhodamine B isothiocyanate (RITC) - dextran (70,000 MW; #R9379) were purchased from Sigma-Aldrich (St. Louis, MO, USA). The antibodies used in this study were obtained from the following sources: Rabbit anti-ZO-1 (#402200) from Invitrogen; mouse anti-Occludin (#331500) from Life Technologies; mouse anti-Glut-1 (#12939), rabbit GFAP (#3670), p-AMPKα (#2535) and AMPKα (#5831) from Cell Signaling Technology; Rabbit anti-ZO-1 (# sc-10804), mouse anti-ICAM-1 (#sc-18853), mouse anti-VCAM-1 (#sc-13160), mouse anti-PECAM-1 (#sc-376764), rabbit anti-Nrf2 (#sc-722), mouse anti-NQO1 (#sc-376023), mouse anti-HO1 (#sc-390991) from Santa Cruz Biotechnology. Donkey anti-rabbit (#NA934) and sheep anti-mouse (#NA931) HRP-linked secondary antibodies were obtained from GE Healthcare (Piscataway, NJ, USA); goat anti-rabbit (#A11008, A21428) conjugated to Alexa Fluor® 488 and 555 respectively and anti-mouse (#A11001, A21422) conjugated to Alexa Fluor® 488 and 555 respectively from Invitrogen (Camarillo, CA, USA).

2.2. Experimental design (in vivo)

The animal protocol for this work was approved by the Institutional Animal Care and Use Committee, TTUHSC, Lubbock, Texas. Sixteen male C57BL/6 J mice, age range 8–10 weeks were purchased from Jackson Laboratories. They were divided into two groups either chronically exposed (via direct inhalation) to cigarette smoke (**CS**) mixed with oxygenated air or oxygenated air alone, 6 times/day; 2 cigarettes/hour, 6–8 h/day, 7 days/week for 2 or 4 weeks following International Organization for Standardization/ Federal Trade Commission (ISO/FTC) standard smoking protocol (35 ml draw, 2 s puff duration, 1 puff per 60 s). CS was generated using a Single Cigarette Smoking Machines (**SCSM**, CH Technologies Inc., Westwood, NJ, USA) following previously published methods [31]. Mice were sacrificed and samples were collected for further analysis. Based on the results, 4 weeks of CS exposure was selected as the time course for a subsequent study to evaluate the protective effects of MF treatment against CS exposure. MF (Sigma, St. Louis, MO, USA) was dissolved in sterile saline at a concentration of 30 mg/ml. MF was administered daily (via intraperitoneal Injections of doses of 100 or 200 mg/kg, 100 mg/kg - **MF100** and 200 mg/kg – **MF200** [28,32]) to mice either exposed to CS (mixed with oxygenated air) or oxygenated air alone (controls) for 4 weeks as earlier mentioned. An equal volume of saline (corresponding to 200 mg/kg MF dose) was used for the control group which received either oxygenated air or CS (mixed with oxygenated air). At the end of the study, mice were sacrificed and samples (plasma and brain) were collected for further analysis.

2.3. Tissue preparation

Mice were sacrificed within an hour of their last CS exposure cycle at the end of the day. Mice were decapitated under anesthesia to collect blood and brain for subsequent biochemical and molecular preparations.

2.4. Cotinine analysis

Plasma and brain homogenate cotinine levels were determined by using Cotinine EIA ELISA kit (1124EB) from OraSure Technologies, Incorporation (PA, USA). Analysis was carried out as per manufacturer's guidelines.

2.5. Glucose analysis

To determine glucose, a tail pin prick was performed on the anesthetized mice and the glucose level was determined using contour next blood glucose meter obtained from Bayer Healthcare (Indiana, USA).

2.6. Cell culture

C57BL/6 mouse primary brain endothelial cells (mBMEC, #C57-6023) were obtained from Cell Biologics (Illinois, USA). mBMEC (passages no. 4−7, obtained from vendor at P3) were seeded on gelatin coated cell culture flasks or glass chamber slides, cultured in recommended medium (M1168) and maintained at 37 ℃ with 5% CO_2 exposure. Apart from primary cells, an immortalized mouse brain endothelial cell line, bEnd.3 (passage no. 22−25, ATCC® CRL-2299™) obtained from ATCC, VA, USA was also used in *in vitro* experiments. Immortalized bEnd.3 endothelial cells were seeded on uncoated cell culture flasks as per manufacturer's protocol and maintained at 37 ℃ with 5% CO_2 exposure. Cell culture medium for bEnd.3 consisted of ATCC- formulated Dulbecco's Modified Eagle's Medium (#30−2002 from ATCC, VA, USA), which was supplemented with 10% FBS (Atlanta Biologicals, GA, USA). The culture medium was changed every other day until the cells reached confluency. Phase contrast microscopy

and the expression of characteristic phenotypic markers confirmed the monolayer integrity of both mBMEC and bEnd.3 cells at confluency. On similar notes primary human brain microvascular endothelial cells (HBMEC, obtained from Cell Biologics) were cultured in accordance with the supplier's protocol.

2.7. Soluble cigarette smoke extract preparation

Soluble CSE was prepared according to the FTC standard smoking protocol (35 ml draw, 2 s puff duration, 1 puff per 60 s) from 3R4F research cigarettes (equivalent to full flavor brands containing 9.4 mg tar and 0.726 mg nicotine per cigarette; University of Kentucky) using a Single Cigarette Smoking Machine (**SCSM**, CH Technologies Inc., Westwood, NJ, USA) following previously published methods [30,33]. CSE solutions were prepared fresh for each cycle and used in culture at a 5% dilution (yielding approximately 100 ng/ml of nicotine).

2.8. Transwell cell culture setup

Clear polyester transwell inserts (Costar® Transwell® polyester membrane cell culture inserts 0.4 µm pore membrane insert; #3470) were seeded with bEnd.3 cells on the luminal side and grown in the culture medium containing DMEM basal media and supplements as mentioned above. The wells were coated with matrigel prior to seeding. Trans-endothelial electrical resistance (TEER) measurement and phase contrast microscopy were used to confirm the confluence and integrity of the cell monolayers.

2.9. Cell viability

MF pretreatment dose for *in vitro* studies were selected based on a MTT cell viability study. In brief, cells cultured in a 96 well plate were pre-treated with varying concentrations of MF and were later treated with 5% CSE for 24 h. Parallel MF untreated controls (with and without 5% CSE) were also assessed for cell viability. Cells were stained with 10 µl of 5 mg/ml tetrazolium MTT (3-(4, 5-dimethylthiazolyl-2)−2, 5-diphenyltetrazolium bromide) for 3 h at 37 °C, after which 100 µl of DMSO (solubilizing agent) was added. The absorbance was read on a Biorad plate reader at a wavelength of 570 nm.

2.10. Treatment (in vitro)

mBMEC and bEnd.3 cells in culture flasks, chamber slides and transwell setup were maintained overnight in respective basal medium (as mentioned earlier) containing 1% FBS with no growth factors (referred to as low serum media). HBMEC cells were seeded in chamber slides for certain studies. These were then exposed to 5% CSE for 24 h (model of mainstream smoke exposure previously described by our group [34]) w/wo MF pretreatment (10–40 µM based on our cell viability results).

2.11. Preparation of protein extracts

Cells were lysed using either RIPA lysis buffer or subcellular protein fractionation kit for cultured cells (Thermo scientific, # 78840) as per manufacturer's guidelines, such that total, nuclear, cytosolic and membrane fractions were collected. For brain tissue lysis, a weighed amount of minced brain was taken in a tube to which ice-cold RIPA lysis buffer (containing protease and Phosphatase inhibitors,15 µl/mg of brain tissue weight) was added. It was homogenized and allowed to stand on a shaker for 30 min. Total protein extract was collected by centrifugation at 14000g for 30 mins. Samples were then aliquoted and stored at −80 °C until needed for protein expression analysis by western blotting.

2.12. Western blotting

Proteins expression was quantified by using Pierce BCA Protein Assay Kit (Thermo Scientific, # 23225). Samples (15−30 µg for cell lysates, 60−90 µg for tissue lysates) were then prepared following method as described in our previous lab report [34]. These denatured samples were run on SDS-PAGE (4−15% gradient gel) and transferred to PVDF membranes for further blotting. Band densities were analyzed by Image Studio Lite Ver 3.1 and calculated as fold change/ percentage change over control protein expression.

2.13. Immunofluorescence

mBMEC, bEnd.3 and HBMEC cells were seeded in two-well chamber slides, grown and treated as mentioned earlier. Cells were fixed (using 16%, methanol free formaldehyde diluted 1 in 4 in 1X PBS; from Polysciences Inc. # 18814), washed and permeabilized (using 0.02% Triton 100X). Cells were then blocked with 5% goat serum in PBS (blocking buffer) at room temperature (RT) for about an hour and incubated with primary antibodies prepared in blocking buffer for overnight at 4 °C. The following day, cells were washed, stained with Alexa Fluor® 488 or 555 conjugated goat anti-rabbit or anti-mouse antibodies or vice-versa at RT and mounted with DAPI in prolonged gold anti-fade mounting media (Invitrogen, OR, USA). Mounted slides upon overnight drying were observed under EVOS digital inverted fluorescence microscope. Cell slides stained with only secondary antibodies served as negative controls [34].

2.14. ELISA

Cell culture supernatants and plasma collected from mice were analyzed by Quantikine ELISA kits (R & D systems, Minneapolis, MN, USA) for quantitative determination of thrombomodulin. The procedure followed was in accordance to the manufacturer's protocol.

2.15. BBB integrity

Our previously reported method [35] was followed to evaluate BBB integrity. Briefly, a mixture of labeled dextrans in PBS (FITC ~4 kDa, 10 mg/ml and RITC ~70 kDa, 10 mg/ml) were added to the luminal compartment of the transwells after 24 h of treatment and exposure to CSE as described earlier in the treatment section. 50 µl of media sample was collected from abluminal compartment. It was replaced with the equal volumes of fresh media to maintain appropriate sink conditions. Baseline permeability coefficients for FITC and RITC under normal conditions were approximately 2.1×10^{-4} cm/s and 5.8×10^{-4} cm/s. Fluorescent measurements were taken at specified excitation and emission wavelengths to determine the concentration of each fluorescent dye in the sample. Appropriate references such as media samples without dextran and that from abluminal compartments of cell free inserts with dextran added to the luminal compartment were taken into consideration during calculations. The permeability measurements were reported as percentage of controls. Further, we also measured TEER (Ω.cm2) using EVOM 2 (World Precision Instruments, Sarasota, FL, USA) to confirm the findings.

2.16. Statistical analysis

Data from all experiments were expressed as mean ± standard mean (SEM) or standard deviation (SD) and analyzed by either *t*-test or one-way ANOVA using GraphPad Prism 6 Software Inc. (La Jolla, CA, USA). Post hoc multiple comparison tests were performed as suggested by the software. P values < 0.05 were considered statistically significant.
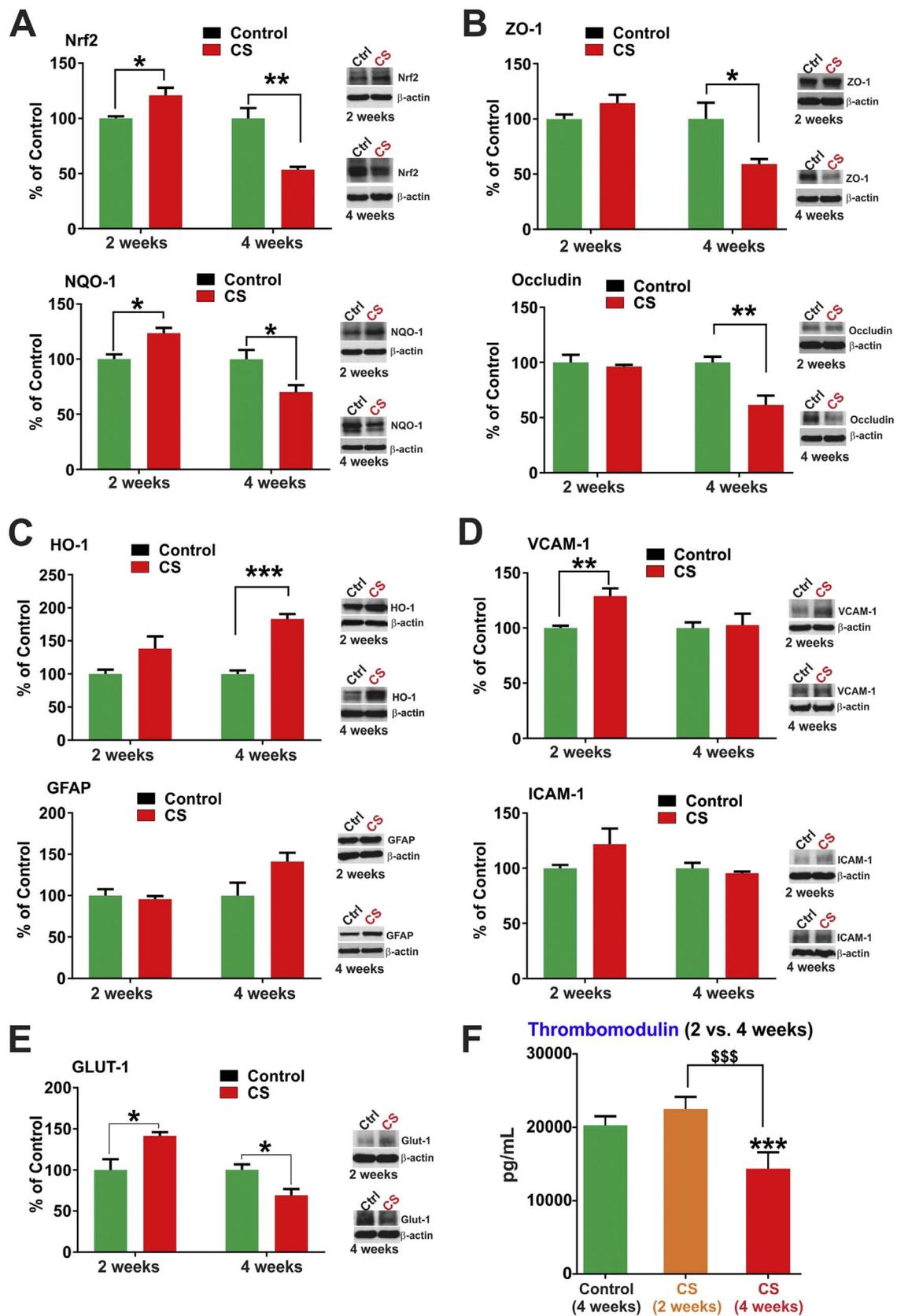
Fig. 1. Effects of CS exposure on anti-oxidant and inflammatory mediators, TJ proteins and thrombomodulin release. Panel A) Prolonged CS exposure (4 weeks) downregulates Nrf2 expression/response and its downstream effector molecule NQO1 and TJ proteins ZO-1 and Occludin (**Panel B**) in mice brain. By contrast, prolonged CS exposure enhanced the expression of HO-1 (significantly) and GFAP (**Panel C**). Initial up-regulation of the inflammatory markers VCAM-1 and ICAM-1 (**Panel D**) normalized back to levels similar to controls upon prolonged CS exposure. Further, prolonged CS exposure (4 weeks) reduced the expression of major glucose transporter Glut-1 (**Panel E**) in mice brain and the levels of thrombomodulin in plasma (**Panel F**). n=4 mice per group. * $p < 0.05$, ** $p < 0.01$, *** $p < 0.001$ vs control; \$\$\$ $p < 0.001$ CS (2 weeks) vs CS (4 weeks). WB analyses report protein/beta actin ratios.

3. Results

3.1. Chronic cigarette smoke exposure promotes cerebrovascular impairment and decreases the plasma level of thrombomodulin

We previously reported that CSE *in vitro* downregulated BBB TJ proteins but also prompted the activation of the cellular antioxidative response system (Nrf2-ARE pathway). Activation of the Nrf2 pathway is indicative of oxidative damages sustained by the BBB endothelium. To understand the effects of CS toxicity *in vivo* at the cerebrovascular level, we analyzed brain lysates from mice chronically exposed to CS via direct inhalation. Plasma cotinine levels were evaluated by ELISA from blood/plasma samples after 4 weeks of CS exposure and was found to be 49.24 ± 4.04 ng/ml. Cotinine levels in brain homogenates was 6 ± 2 ng/ml. Western blot analysis of the whole brain homogenate from C57BL6/J mice that were exposed to CS revealed an initial increase in Nrf2 and its downstream protein NQO1 expression (at 2 weeks, $p < 0.05$) followed by a significant decrease in its expression at 4 weeks ($p < 0.01$ for Nrf2, $p < 0.05$ for NQO-1, Fig. 1**A**). While ZO-1 and occludin expression levels were practically unchanged following 2 weeks of chronic CS exposure, downregulation of these TJ proteins became markedly evident in mice chronically exposed to CS for 4 weeks as demonstrated by the WB analysis. In addition to ZO-1, occludin expression levels were also significantly downregulated at 4 weeks exposure ($p < 0.01$; see Fig. 1**B**). Similarly, 2 weeks of CS exposure did not significantly alter HO-1 (modest increase) and GFAP expression however, both stress markers were substantially upregulated at 4 weeks of CS exposure ($p < 0.001$; see Fig. 1**C**). By contrast, the expression levels of inflammatory adhesion molecules VCAM1 ($p < 0.01$) and ICAM1 were upregulated following 2 weeks of CS exposure but remained unchanged at 4 weeks' time point (Fig. 1**D**). Noteworthy was the upregulation of the glucose transporter Glut-1 following 2 weeks of CS exposure ($p < 0.05$) which however, reversed at 4 weeks exposure ($p < 0.05$, Fig. 1**E**). On a similar pattern, 2 weeks of CS exposure caused a slight increase in plasma levels of the anticoagulant protein thrombomodulin which reversed at 4 weeks' exposure becoming significantly downregulated ($p < 0.0001$; see Fig. 1**F**).

3.2. Metformin prevents cigarette smoke-induced loss of BBB integrity and function both in vitro and in vivo

MTT cytotoxicity studies were used to assess MF dosing based on its impact on cell viability (using bEnd.3 cells) w/wo concomitant exposure to CSE. As shown in Fig. 2**A**, 24 h continuous exposure to different MF doses w/wo CSE did not cause any significant cellular toxicity (except for the 5 mM dosing) as demonstrated by MTT assay. Thus based on these results and literature evidence the MF working dose [36] for all our *in vitro* studies was finalized at 10 μM which corresponds approximately to half the plasma concentration of MF. Immunofluorescence and Western blot analyses demonstrated that CSE in mBMEC cells enhanced the expression levels of the oxidative/inflammatory stress markers HO-1 and PECAM-1 while downregulating that of tight junction proteins ZO-1 ($p < 0.01$) and occludin ($p < 0.05$) (vs. controls) (Fig. 2**B2** and **C**). Notably, these adverse changes were countered by MF pretreatment ($p < 0.01$, Fig. 2**B** and **C**). Although the total levels of Nrf2 in mBMEC cells remained unaltered in response to CSE exposure, its nuclear translocation was significantly enhanced (Fig. 2**B1**). Also in cells exposed to CSE and pre-treated with MF both the increased expression level and nuclear translocation on Nrf2 were clearly evident. This resulted in an overall increase of Nrf2 nuclear activity which was evidenced by a comparable increase in the expression level of NQO-1 (downstream product of Nrf2-ARE pathway of activation; $p < 0.05$) coupled with renormalization of ZO-1 and Occludin expression levels as further evidenced by immunofluorescent analysis of the cell monolayers (Fig. 2**C and** S1). From a functional point of view, CSE negatively impacted BBB integrity as expected (also

based on CSE effect on TJ protein expression) however its harmful effect was negated by MF treatment ($p < 0.0001$) as clearly shown by the TEER measurements (Fig. 2**D**) and confirmed by the parallel increase in permeability to FITC and rhodamine conjugated dextran molecules (paracellular markers [29]). Further, CSE exposure significantly decreased the endothelial release of the anticoagulant factor thrombomodulin ($p < 0.05$) and these effect was offset by MF as shown in Fig. 2**E**.

Following *in vivo* studies (as rationalized in Fig. 3**A**) were performed to assess and validate the protective effect of MF against impairment of the BBB and cerebrovascular functions caused by CS exposure. Initial tests were performed to assess whether MF dosing had any negative impact on body weight and glucose levels. For this purpose mice were regularly weighed and tested for fasting blood glucose levels. As shown in Fig. 3**B**, there was a significant increase ($p < 0.05$) in weight in control group receiving either saline or 100 mg/kg metformin i.p. over a time period of 4 weeks. Note however, that there were no differences in body weight within the groups on day 0 or after termination of the study at 4 weeks' time point (see Fig. 3**B** top panels). Further, fasting blood glucose levels across the groups were within limits with no significant inter group differences either at 2 or 4 weeks' time points indicating the neither MF nor CS exposure influenced these safety parameters in any significant way. To evaluate the cerebrovascular and BBB impact of the MF treatments and CS exposure, we performed western blot analysis for Nrf2, NQO-1, Glut-1, ZO-1 and Occludin (all were downregulated following 4 weeks of CS exposure as shown in Fig. 1**A** to **E**). Our results indicate that both 100 mg/kg and 200 mg/kg of MF were sufficient to counteract CS' adverse effects (see Fig. 4**A**) by preventing the downregulation of ZO-1 ($p < 0.05$ for CS+MF100, $p < 0.0001$ for CS+MF200), Occludin ($p < 0.001$ for CS+MF100, $p < 0.001$ for CS+MF200), Nrf2 ($p < 0.05$ for CS+MF100, $p < 0.01$ for CS+MF200) and NQO-1 ($p < 0.01$ for CS+MF100, $p < 0.001$ for CS+MF200). The protective effects were dose dependent. Also MF prevented downregulation of the glucose transporter Glut-1 by CS and the effect was also dose dependent. Interestingly, western blot analysis of brain homogenate from our *in vivo* studies revealed an increase in AMPK phosphorylation in response to CS exposure which was enhanced in a dose-dependent fashion by pre-treatment with MF ($p < 0.05$ Ctrl vs CS+MF100, $p < 0.01$ Ctrl vs. CS+MF200 and $p < 0.05$ CS+MF100 vs CS+MF200) (Fig. 4**B**).

Also noteworthy is the fact that MF (both **MF100** and **MF200**) prevented CS-induced downregulation of thrombomodulin levels ($p < 0.05$ for CS+MF100, $p < 0.01$ for CS+MF200, Fig. 4**C**). Note however, that these doses are approximately 0.45 (MF100) to 0.9 (MF200) the maximum recommended human daily dose of 2000 mg based on body surface area comparisons.

3.3. Nrf2 activation by MF enhances ZO-1 and Glut-1 protein expression and is independent of AMPK phosphorylation

WB analysis of whole brain homogenate from MF-treated mice only revealed a significant increase in the expression level of Nrf-2 both MF100 and MF200 mice ($p < 0.01$ Ctrl vs MF100 or MF200, Fig. 5**A**) when compared to controls (saline only) although, corresponding increase in NQO-1 expression levels where statistically significant ($p < 0.01$ Ctrl vs MF200, $p < 0.01$ MF100 vs MF200) only at the higher MF dosing. Similar to *in vitro*, MF increased the protein expression level of ZO-1 ($p < 0.05$ Ctrl vs MF100, $p < 0.01$ Ctrl vs MF200, $p < 0.05$ MF100 vs MF200, Fig. 5**A**) and Occludin ($p < 0.05$ Ctrl vs MF100 or MF200) however, in the case of ZO-1 the responses were dose dependent but not for Occludin. An MF dose-dependent increase of Glut-1 expression was also observed although was not statistically significant. Further, phosphorylation of AMPK was only observed with MF200 ($p < 0.01$ Ctrl vs MF200).

To understand the inter-relation between Nrf2, Glut-1 and ZO-1 expression, parallel mBMEC cell cultures were treated with sulfora-
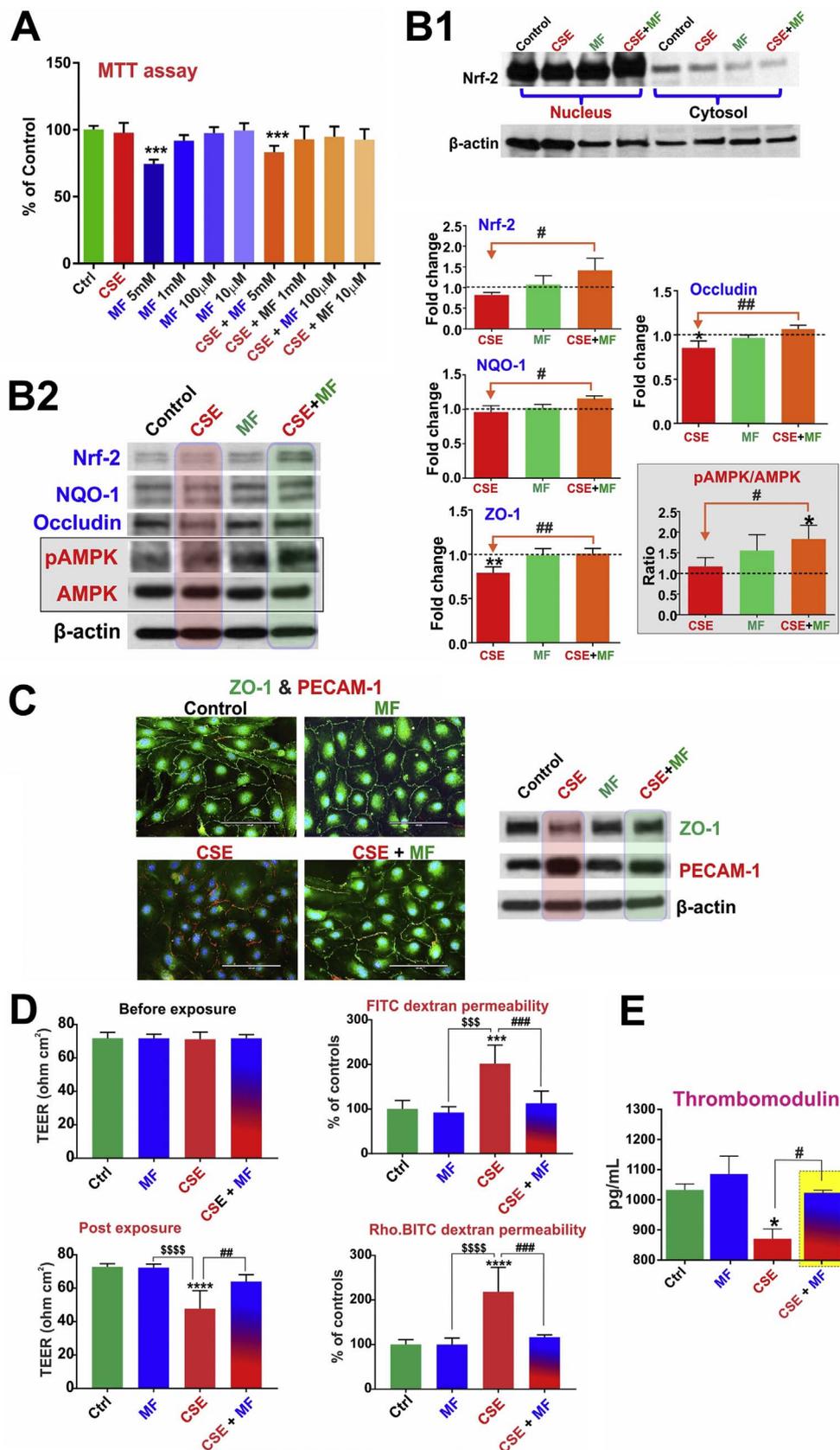
Fig. 2. Protective effects of MF against CSE induced BBB endothelial cell dysfunction. Panel A: MTT cytotoxicty assay for MF dose evaluation. **Panel B** and **C**: MF activates Nrf2 pathway as demonstrated by its increased nuclear translocation (**B1**). This resulted in an increased expression of the TJ proteins ZO-1 and Occludin as well as the pAMPK/AMPK ratio (**B2**) in comparison to cells treated with CSE. Concurrently, the expression level of the inflammatory marker PECAM-1 was downregulated (**C**). **Panel D**: MF prevents the decrease in TEER or increase in dextran permeability due to CSE exposure. **Panel E:** MF also restores the thrombomodulin release from endothelial cells which decreased upon CSE exposure. n=3 to 4 biol. rep. * p < 0.05, ** p < 0.01, *** p < 0.001, p < 0.0001 vs control; $$$p < 0.001, $$$$p < 0.0001 MF vs CSE; #p < 0.05, ## p < 0.01, ### p < 0.001 CSE vs CSE+MF. WB analyses report protein/beta actin ratios.
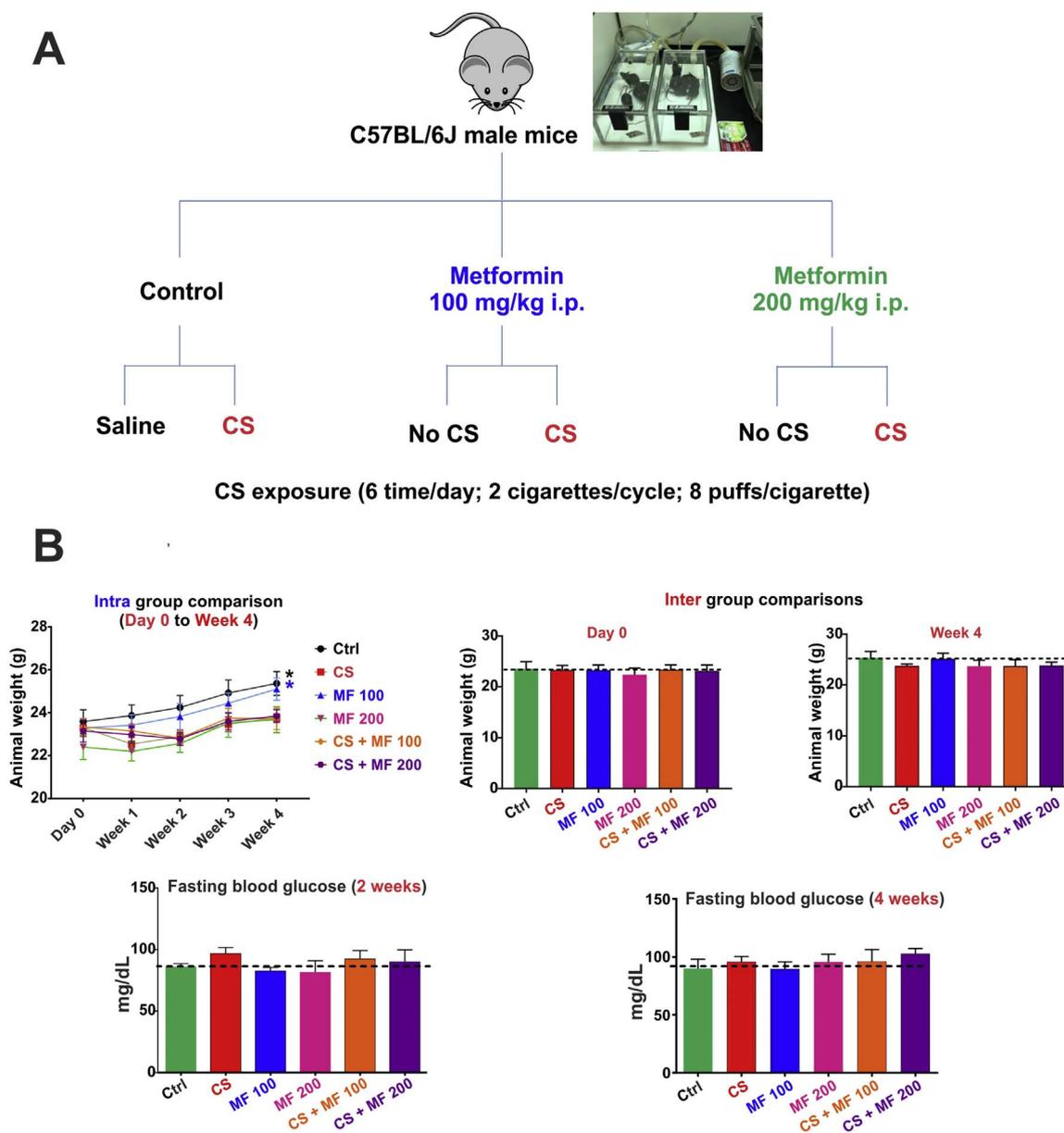
Fig. 3. MF-CS study experimental plan and safety profile. Panel A illustrates the experimental design of the in vivo study evaluating protective effect of MF against CS- induced cerebrovascular impairment. **Panel B:** Effect of saline/MF treatments with / without CS exposure on body weight and fasting glucose levels in vivo. N=4 to 6 mice per group, p < 0.05 week 4 vs day 0.

phane (**SFN**; an established Nrf-2 activator [37,38]) 5 μM. Immunofluorescence imaging revealed an increase in both ZO-1 and Glut-1 expression (Fig. 5**B1**) in SFN treated cells in comparison to controls. Effects on Glut-1 expression where further verified by western blotting as shown in Fig. 5**B2**. Using different doses of MF (10 μM, 20 μM and 40 μM) we reproduced a corresponding upregulation in the expression levels of Nrf2 (including nuclear translocation), NQO-1, Glut-1 and ZO-1 (Fig. 5**C and** S2). These concentrations are within the plasma levels measured in patients with the exception of 40 μM which is above these values [39]. To determine whether MF-induced Nrf2 upregulation and nuclear translocation was linked to the activation of AMP-activated protein kinase (**AMPK**), we performed immunofluorescence imaging on cells exposed to compound C (a well-known AMPK inhibitor [40]) with or without MF. As shown in Fig. 5**D** MF increased the expression of Nrf2 (including its nuclear translocation) and that of its downstream product NQO-1 unhindered by the presence of compound C.

4. Discussion

A key regulator of redox homeostasis in inactive cells, Nrf2 exerts cytoprotective functions encompassing anti-oxidative and anti-inflammatory responses under physiological conditions [41]. Absence of Nrf2 has been shown to exacerbate brain injury with increased susceptibility to brain edema and BBB breakdown [42]. Effects of CS in relation to Nrf2 have been heavily investigated in terms of pulmonary responses. In comparison to wild-type mice, Nrf2 deficient mice exposed to CS for 6 months were associated with more pronounced oxidative stress and bronchoalveolar inflammation leading to early onset and extensive emphysema [43]. Clinically, Nrf2 protein levels were found to be significantly downregulated in both cytosol and nuclei in biopsy-derived human lung tissue, in whole lung tissue samples and alveolar macro phages from smokers with emphysema in comparison to smokers and nonsmokers without emphysema [44]. Further, results from our previous reports have shown that Nrf2 regulates BBB endothelial tight and adherence junction protein expressions [29],
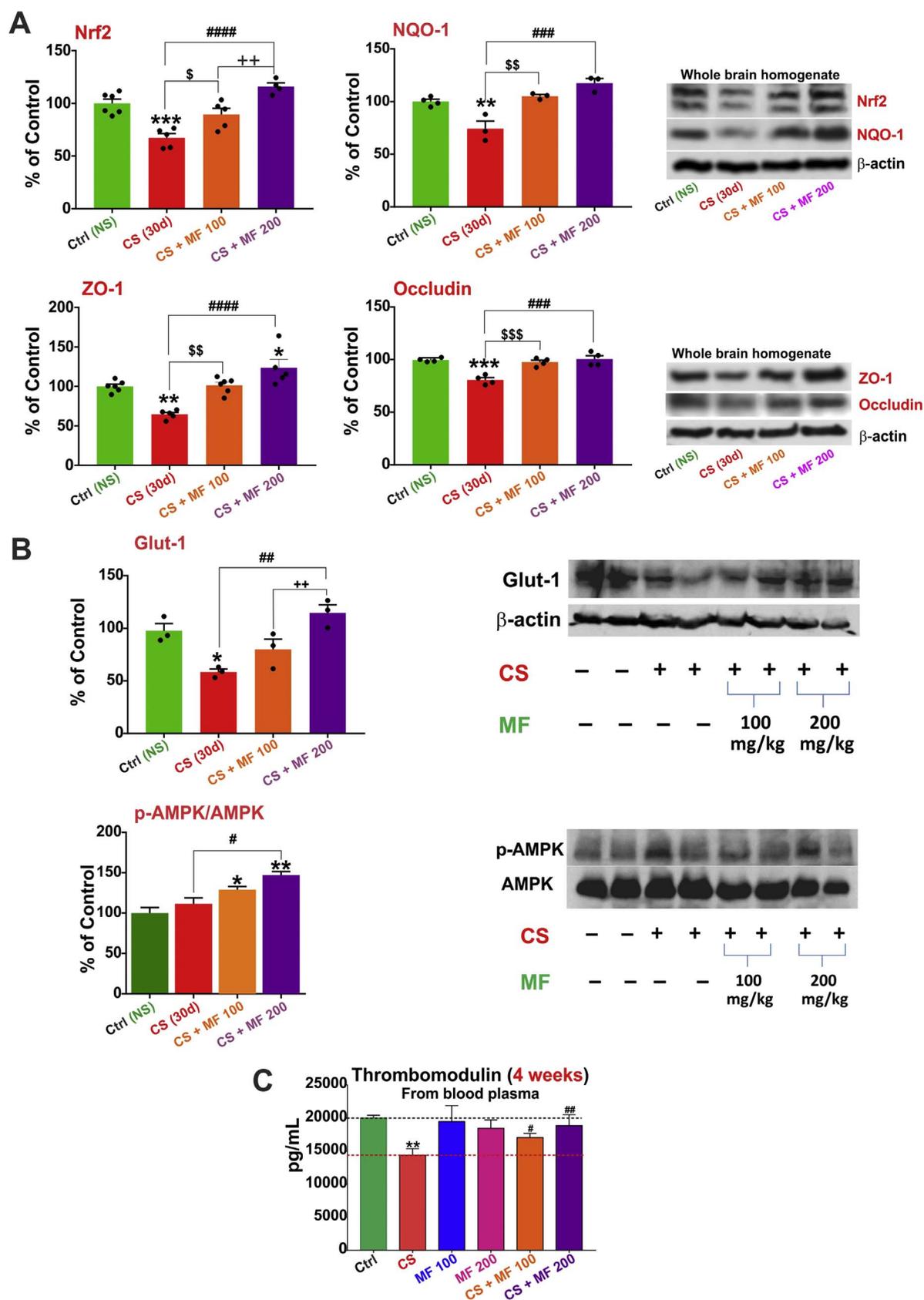
Fig. 4. MF-CS study in vivo findings. In vivo data demonstrating that downregulation of total brain levels of Nrf2, NQO-1 ZO-1, Occludin (**Panel A**), Glut-1(**Panel B**) and thrombomodulin (**Panel C**) in the blood plasma by chronic TS exposure can be restored by MF in a dose-dependent manner (100 and 200 mg/kg). Further, a dose dependent phosphorylation by MF in CS exposed mice brain was also observed (**Panel C**). n=4–6 biol. rep. * p < 0.05, ** p < 0.01, *** p < 0.001, p < 0.0001 vs control; $ p < 0.05, $$ p < 0.01, $$$ p < 0.001 CS vs CS+MF 100; #p < 0.05, ## p < 0.01, ### p < 0.001, #### p < 0.0001 CS vs CS+MF 200 and ++p < 0.01 CS+MF 100 vs CS+MF 200.
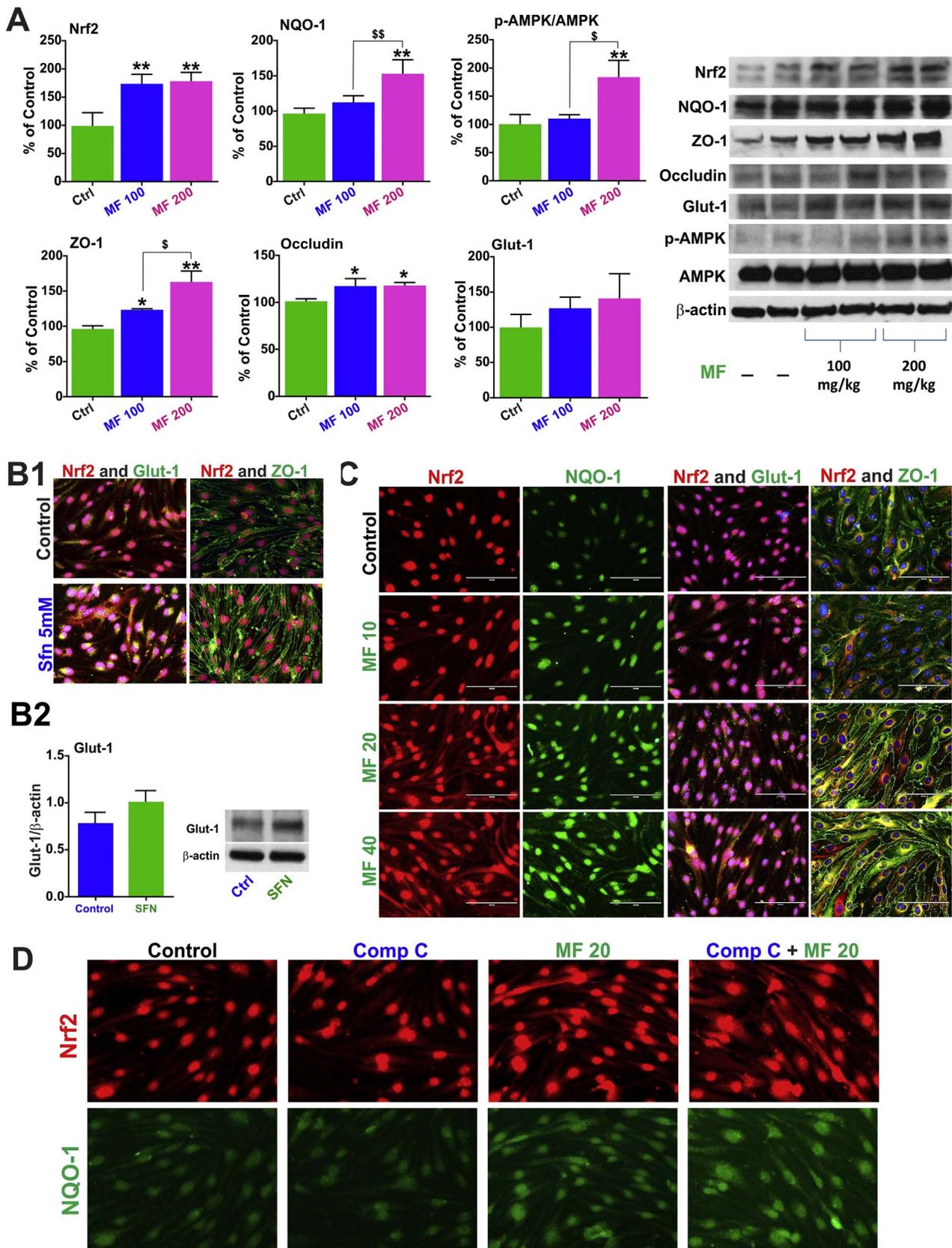
Fig. 5. Nrf2 and AMPK interplay. Panel **A** shows the effect of MF alone in vivo in comparison to controls. Notably the increase in ZO-1 and Glut-1 in relation to Nrf2 was reproduced in mBMEC cells using sulforaphane (P**anel B**). Further, a dose dependent increase in NQO-1, Glut-1 and ZO-1 was observed with MF (0–40 μM) treatment in mBMEC cells by immunofluorescence imaging (**Panel C**). Compound C pre-treatment did not inhibit the upregulation of Nrf2 upon MF treatment in mBMEC cells as shown in the immunofluorescence images (**Panel D**).

indicating that increased and persistent levels of oxidative stress that adversely impact Nrf2 levels can negatively influence BBB function and integrity. Thus, the effects of prolonged CS exposure on Nrf2, its downstream proteins and tight junction proteins (such as ZO-1 and Occludin) observed in our study strongly support these previous observations. Results from this study demonstrate a progressive down-regulation of Nrf2, NQO-1, ZO-1 and Occludin in total brain homogenates *in vivo* following 4 weeks of CS exposure, although an initial cytoprotective increase of Nrf2, NQO-1 and ZO-1 expressions was observed after 2 weeks of chronic CS exposure (Fig. 1), the negative impact of CS on these same targets was keenly noticeable at 4 weeks' time point. Importantly, a similar biphasic trend of increase followed by a decrease in Glut-1 expression was observed in 4 weeks CS-exposed mice vs. 2 weeks groups (Fig. 1). While activation of the transcription factor Nrf2 is well known to be one of the major cellular defense lines against oxidative and xenobiotic stress, its influences on genes involved in lipid and glucose metabolism has also been recently established. Heiss and colleagues [45] have demonstrated that availability of glucose is a decisive factor for Nrf2-mediated gene expression, which detrimentally influence the outcome in many models of disease, including cancer, vascular disease, type II diabetes or neurodegenerative disorders. In fact, there are studies demonstrating that the absence of Nrf2 worsens the diabetic phenotype in mice; and that impairment in endothelial glucose uptake downregulates tight junction protein expression [46]. Thus, it is not surprising to observe a similar pattern of biphasic trend in expression of Glut-1, Nrf2 and ZO-1 levels upon CS exposure. Although HO-1 (an oxidative stress marker) is considered to be one of the downstream proteins of Nrf2 activation (Nrf2-ARE pathway), its induction has also been reported to be Nrf2 independent [47,48]. HO-1 activity is significantly increased both *in vitro* and *in vivo* upon exposure to cytokines, hypoxia, heme, metals, xenobiotics, endocrine factors, tobacco smoke and multiple oxidative stressors [49]. Similarly, gliogenesis marked by significant increase in GFAP (reactive astrocytosis) is evident upon abnormal aggregation of the protein and concomitant cerebrovascular toxicity due to oxidative stress [50,51]. Interestingly, both HO-1 and GFAP increased upon prolonged CS exposure (4 weeks) indicating higher levels of oxidative stress. Inflammatory mediators such as VCAM-1 and ICAM-1 were upregulated upon acute CS exposure (2 weeks). However, there expressions returned to those similar to controls upon further CS exposure. This data is in line with the earlier reported *in vivo* works wherein a decrease of endurance capacity and systemic inflammation was noticed upon prolonged smoke exposure (32 weeks) in mice [52]. Measurements of protein expression levels in whole brain homogenate does not allow us to specifically assess the impact of CS exposure on the vascular endothelium and although some of the proteins we measured are fairly specific to the endothelium such as ZO-1, occludin, Glut-1, VCAM, ICAM; nrf-2, HO-1, NQO-1 are ubiquitously expressed. This indicates that the impact of CS on the Nrf2-ARE system spreads to the all brain tissue. However, concerning the specific impact on the BBB, our in vitro data (Supplementary Fig. 1) clearly show that chronic CS exposure does indeed decrease Nrf2 and ZO-1 expression in primary human brain microvascular endothelial cells. Taken together, our data indicate that prolonged CS exposure increases oxidative stress, thereby compromising the Nrf2-ARE anti-oxidant pathway and causing cerebrovascular impairment in terms of loss of tight junction proteins such as ZO-1, occludin and glucose transporter such as Glut-1. Thus, these in vivo studies provide a good indication of the chronic effects of CS exposure.

Metformin has lately been established to act by both AMPK dependent and independent mechanisms [53]. Montalvo and his colleagues showed that metformin treatment provides benefits of calorie restriction by increase in AMPK activation and antioxidant activity resulting in increased lifespan and improved health span of aging mice [32]. Furthermore in separate studies, pre-treatment with MF was also found to prevent ischemia induced brain injury by

activation of AMPK and Nrf2 pathway and promotion of ZO-1, occludin and claudin-5 rearrangement [27,28]. In the present study, we demonstrated that pretreatment with MF *in vitro* prevented CSE-induced tight junction protein (ZO-1 and occludin) downregulation and induced Nrf2 and AMPK pathway activation, although, our data suggest that activation of Nrf2 (upregulation and nuclear translocation) is not strictly linked to that of AMPK activation. In fact data reported in Fig. 4A and B show that in CS exposed mice Nrf2 downregulation (Fig. 4A) is in opposition with a slightly increase of AMPK activation (Fig. 4B) caused by CS. Also MF-induced Nrf2 upregulation in CS exposed mice is clearly dose dependent (Fig. 4A) while that of AMPK activation is not (observed only at MF highest dose; Fig. 4B) and as shown in Fig. 5C, blockade of AMPK activity by the use of compound C did not hinder the ability of MF to upregulate Nrf2 expression and nuclear translocation. Thus it is possible that additional pathway-specific mediators/facilitators may be involved in these processes. We also observed an inhibition in membrane expression of pro-inflammatory mediator PECAM-1 in MF pre-treated cells exposed to CSE vs CSE-free cultures (Fig. 2). These observed effects are well in line with our previously published *in vitro* study showing that CSE contains high concentrations of NO and hydrogen peroxide causing cellular oxidative stress and loss of BBB endothelial cell function [30,34]. Additionally, CSE-induced reduction in ZO-1 and occludin expression was accompanied by a loss of BBB integrity as demonstrated by the TEER decrease of the endothelial monolayers (in transwell set-ups) and the parallel increase in paracellular permeability to both 4 and 10 kDa labeled dextrans (Fig. 2D). This suggests a loss of selective permeability to low molecular weight paracellular markers although it is possible that restriction to the passage of larger polar compounds remained intact. Importantly, MF pre-treatment countered the CSE impact on BBB permeability (Fig. 2D), thus implicating a possible cerebrovascular protective effect in smokers.

Metformin is a glucose lowering agent and is also known to inhibit weight gain [53]. Furthermore, TS is also known to cause a loss in appetite leading to lower body weight [54]. Therefore a time dependent body weight and fasting blood glucose analysis was carried out to understand whether MF administration or/and CS exposure had any synergistic detrimental effects on these health parameters. Our data indicate that control mice receiving either saline or MF followed a regular trend in increase in body weight. Even though the remaining groups did not show a similar trend, no loss of body weight was observed either, thus demonstrating that the MF dosing and the levels of CS exposure did not have any relevant safety impact on the animals. This was also demonstrated by the lack of significant changes in fasting blood glucose levels we observed in tests vs. control animals (Fig. 3). As for the protective effects of MF administration against CS induced cerebrovascular impairment, a dose dependent restoration and increase in Nrf2 levels were observed in brain homogenates of MF treated CS exposed mice in comparison to untreated CS exposed mice. Similar restoration/prevention of CS induced downregulation of NQO-1, Glut-1 and tight junction proteins ZO-1 and occludin were also observed at the cerebrovascular level in CS exposed mice treated with MF (Fig. 4). These novel data clearly indicate that metformin is capable in preventing CS induced cerebrovascular dysfunction and should be further explored clinically to improve healthspan and lifespan of ex-smokers or possibly people exposed to second hand smoke. The protective nature of Nrf2 may be altered in smokers by means of somatic mutation, epigenetic alteration, and accumulation of disruptor proteins, thereby promoting cell resistance and proliferation of cancerous cells as indicated by many studies [55,56].

Even though our experiments model chronic CS exposure, the adverse effects of CS we observed may not fully recapitulate those experienced by chronic smokers who have been exposed to CS (either first or second hand exposure) for many years (decades). Comparable long term experimental conditions would be unfeasible in a laboratory setting. Nevertheless the beneficial effects of MF against CS-induced

cerebrovascular damages should also be assessed and explored in a clinical setting for ex-smokers and second hand smokers at lower risks for Nrf2 mutation. Epigenetic studies focusing Nrf2 mutations and their impact on cellular function should also be undertaken. Further, in relation to the impact of Nrf2 on TJ expression and BBB integrity is it unclear whether this is a direct effect of Nrf2 mediated by the activation of the Nrf2-ARE pathway or these are secondary effects related to prevention of protein degradation by oxidative stress. Previous studies by Shintani et al. on airway epithelial barrier integrity suggest that a direct effect is indeed possible [57] which is in line with our in vitro data using either sulforaphane or MF to enhance Nrf2 expression (see Fig. 5**B**1 and **C**). However, this does not rule out the possibility that a concomitant secondary effects related to prevention of TJ degradation by oxidative stress is also in place and further studies will be needed to elucidate these mechanisms of action.

Smoking can elicit hemostatic activation and thrombosis by several mechanisms including reduction in the release of anti-coagulant factors such as thrombomodulin from endothelial cells. Lack of thrombomodulin can severely impact the anticoagulant feature of thrombin (through activation of Protein C [58]) and negatively impact the ability to control the coagulation cascade. This can lead to increased risk of blood clot formations and stroke as observed in smokers. In fact, our data clearly show that CS (and CSE *in vitro*) exposure significantly decreased in the vascular levels of thrombomodulin both in vitro (Fig. 1**F**) and in vivo (Fig. 2**E**). In both cases, lowering of thrombomodulin levels by CS (or CSE) was prevented by MF. This suggests the possible use of MF as a therapeutic/prophylactic venue to prevent/reduce smoking-dependent cerebrovascular damage and reduce the risk and severity of stroke in both chronic smoker and early stage former smokers who are still at high risk of stroke.

AMPK is a ubiquitously expressed energy sensing enzyme which is activated by increases in the AMP to ATP ratio [59], occurring in various stress conditions such as hypoxia, ischemia and CS [60]. Increased susceptibility to lung inflammation (increased levels of cytokines such as IL-8) and emphysema were observed in AMPKα1-deficient mice upon CS exposure, implying a pivotal role played by AMPK in reducing lung inflammation and emphysema [61]. We observed AMPK activation in mice brain upon CS exposure (Fig. 5). Furthermore, MF a known activator of AMPK pathway was also found to increase the phosphorylation of AMPK in a dose dependent manner (Fig. 5). We also observed that MF alone increased Nrf2, its downstream detoxification protein NQO-1, Glut-1 and tight junction proteins ZO-1 and occludin (Fig. 5); thereby further validating a positive relation between Nrf2 redox pathway, metabolic pathway and cerebrovascular integrity. A similar relation was observed upon cellular treatment with known Nrf2 activator- sulforaphane [37] and MF (dose-dependent) which increased Glut-1 and ZO-1 expression along with promoting Nrf2 activation (see Fig. 5). In light of the emerging interplay between redox and metabolic signaling pathways, several articles have reported the existence of a potential positive cross talk between Nrf2 and AMPK pathways [62–64]. As previously mentioned above, we observed that prolonged CS exposure (4 weeks) minimally increases phosphorylation of AMPK (Fig. 2**B**2) but substantially decreases the total level of Nrf2 and its downstream protein NQO-1 (Figs. 1 and 4). Further, while MF increases Nrf2 expression at each concentration we tested in vivo, only the highest one (200 mg/Kg) elicited AMPK activation. In view of these results the Nrf2 and AMPK pathways seem to share limited cross-talking and perhaps other pathway specific modulators/promoters may be implicated (e.g., insulin [40]). Supporting this hypothesis, we also observed that compound C, an established inhibitor of AMPK phosphorylation did not inhibit Nrf2 upregulation by MF treatment (Fig. 5**D**). Nonetheless, our data taken together demonstrate protective effects of MF against CS- induced cerebrovascular impairment by both activation of Nrf2 and AMPK pathway which seems to be independent of each other in this scenario.

In conclusion, this study emphasizes the critical role of Nrf2 in maintaining healthy cerebrovascular conditions and BBB endothelial structure and functional integrity. Our data suggests that CS significantly impairs the cerebrovascular condition and endothelial function by increased load of oxidative stress due to altered Nrf2 signaling. Metformin notably counteracts these CS- induced adverse effects through modulation of Nrf2 expression and helps in restoring the cerebrovascular homeostasis. Thereby, strategies to augment Nrf2 activity could hold therapeutic potential to prevent CS- induced cerebrovascular dysfunction. In addition, we also provide a mechanistic insight regarding the interplay of Nrf2 and AMPK pathway which seems to be more independent than expected.

Acknowledgements

Appendix A. Supporting information

Supplementary data associated with this article can be found in the online version at doi:10.1016/j.redox.2017.02.007.

References

[1] Who Report on the Global Tobacco Epidemic, 2013, Ref Type: Generic, 2013.
[2] The Health Consequences of Smoking-50 Years of Progress: A Report of the Surgeon General. 2014.
[3] Fast Facts. 12–20–2016. Ref Type: Online Source.
[4] I.M. Cojocaru, M. Cojocaru, V. Sapira, A. Ionescu, Evaluation of oxidative stress in patients with acute ischemic stroke, Rom. J. Intern. Med. 51 (2013) 97–106.
[5] Health Effects of Cigarette Smoking. 12–1–2016. Ref Type: Online Source.
[6] How Tobacco Smoke Causes Disease: The Biology and Behavioral Basis for Smoking-Attributable Disease: A Report of the Surgeon General. Chapter 3. Publications and Reports of the Surgeon General 2010.
[7] M. Hossain, T. Sathe, V. Fazio, P. Mazzone, B. Weksler, D. Janigro, et al., Tobacco smoke: a critical etiological factor for vascular impairment at the blood-brain barrier, Brain Res. 1287 (2009) 192–205.
[8] P. Naik, N. Fofaria, S. Prasad, R.K. Sajja, B. Weksler, P.O. Couraud, et al., Oxidative and pro-inflammatory impact of regular and denicotinized cigarettes on blood brain barrier endothelial cells: is smoking reduced or nicotine-free products really safe?, BMC Neurosci. 15 (2014) 51.
[9] H.W. Chen, M.L. Chien, Y.H. Chaung, C.K. Lii, T.S. Wang, Extracts from cigarette smoke induce DNA damage and cell adhesion molecule expression through different pathways, Chem Biol. Inter. 150 (2004) 233–241.
[10] J.S. Gill, M.J. Shipley, S.A. Tsementzis, R. Hornby, S.K. Gill, E.R. Hitchcock, et al., Cigarette smoking. A risk factor for hemorrhagic and nonhemorrhagic stroke, Arch. Intern. Med. 149 (1989) 2053–2057.
[11] K. Panda, R. Chattopadhyay, M.K. Ghosh, D.J. Chattopadhyay, I.B. Chatterjee, Vitamin C prevents cigarette smoke induced oxidative damage of proteins and increased proteolysis, Free Radic. Biol. Med. 27 (1999) 1064–1079.
[12] S.T. Hanna, Nicotine effect on cardiovascular system and ion channels, J. Cardiovasc. Pharmacol. 47 (2006) 348–358.
[13] L. Wang, M. Kittaka, N. Sun, S.S. Schreiber, B.V. Zlokovic, Chronic nicotine treatment enhances focal ischemic brain injury and depletes free pool of brain microvascular tissue plasminogen activator in rats, J. Cereb. Blood Flow Metab.: Off. J. Int. Soc. Cereb. Blood Flow Metab. 17 (1997) 136–146.
[14] J.R. Paulson, T. Yang, P.K. Selvaraj, A. Mdzinarishvili, C.J. Van der Schyf, J. Klein, et al., Nicotine exacerbates brain edema during in vitro and in vivo focal ischemic conditions, J. Pharm. Exp. Ther. 332 (2010) 371–379.
[15] C. Heeschen, M. Weis, J.P. Cooke, Nicotine promotes arteriogenesis, J. Am. College Cardiol. 41 (2003) 489–496.
[16] D.F. Catanzaro, Y. Zhou, R. Chen, F. Yu, S.E. Catanzaro, M.S. De Lorenzo, et al., Potentially reduced exposure cigarettes accelerate atherosclerosis: evidence for the role of nicotine, Cardiovasc. Toxicol. 7 (2007) 192–201.
[17] S. Das, N. Gautam, S.K. Dey, T. Maiti, S. Roy, Oxidative stress in the brain of nicotine-induced toxicity: protective role of Andrographis paniculata Nees and vitamin E, Appl. Physiol. Nutr. Metab. 34 (2009) 124–135.
[18] Y. Arnson, Y. Shoenfeld, H. Amital, Effects of tobacco smoke on immunity, inflammation and autoimmunity, J. Autoimmun. (2009).
[19] J.C. Will, D.A. Galuska, E.S. Ford, A. Mokdad, E.E. Calle, Cigarette smoking and diabetes mellitus: evidence of a positive association from a large prospective cohort study, Int. J. Epidemiol. 30 (2001) 540–546.
[20] C. Willi, P. Bodenmann, W.A. Ghali, P.D. Faris, J. Cornuz, Active smoking and the

risk of type 2 diabetes: a systematic review and meta-analysis, JAMA 298 (2007) 2654–2664.

[21] F. Giacco, M. Brownlee, Oxidative stress and diabetic complications, Circ. Res. 107 (2010) 1058–1070.

[22] W.H. Hoffman, S.M. Stamatovic, A.V. Andjelkovic, Inflammatory mediators and blood brain barrier disruption in fatal brain edema of diabetic ketoacidosis, Brain Res. 1254 (2009) 138–148.

[23] K.E. Wellen, G.S. Hotamisligil, Inflammation, stress, and diabetes, J. Clin. Investig. 115 (2005) 1111–1119.

[24] P. Naik, L. Cucullo, Pathobiology of tobacco smoking and neurovascular disorders: untied strings and alternative products, Fluids Barriers CNS 12 (2015) 25.

[25] M.C. Polidori, G. Nelles, Antioxidant clinical trials in mild cognitive impairment and Alzheimer's disease - challenges and perspectives, Curr. Pharm. Des. 20 (2014) 3083–3092.

[26] S. Prasad, R.K. Sajja, J.H. Park, P. Naik, M.A. Kaisar, L. Cucullo, Impact of cigarette smoke extract and hyperglycemic conditions on blood-brain barrier endothelial cells, Fluids Barriers CNS 12 (2015) 18.

[27] G. Ashabi, L. Khalaj, F. Khodagholi, M. Goudarzvand, A. Sarkaki, Pre-treatment with metformin activates Nrf2 antioxidant pathways and inhibits inflammatory responses through induction of AMPK after transient global cerebral ischemia, Metab. Brain Dis. (2014).

[28] Y. Liu, G. Tang, Y. Li, Y. Wang, X. Chen, X. Gu, et al., Metformin attenuates blood-brain barrier disruption in mice following middle cerebral artery occlusion, J. Neuroinflamm. 11 (2014) 177.

[29] R.K. Sajja, K.N. Green, L. Cucullo, Altered Nrf2 signaling mediates hypoglycemia-induced blood-brain barrier endothelial dysfunction in vitro, PLoS One 10 (2015) e0122358.

[30] P. Naik, R.K. Sajja, S. Prasad, L. Cucullo, Effect of full flavor and denicotinized cigarettes exposure on the brain microvascular endothelium: a microarray-based gene expression study using a human immortalized BBB endothelial cell line, BMC Neurosci. 16 (2015) 38.

[31] P. Naik, N. Fofaria, S. Prasad, R.K. Sajja, B. Weksler, P.O. Couraud, et al., Oxidative and pro-inflammatory impact of regular and denicotinized cigarettes on blood brain barrier endothelial cells: is smoking reduced or nicotine-free products really safe?, BMC Neurosci. 16 (2015) 51.

[32] A. Martin-Montalvo, E.M. Mercken, S.J. Mitchell, H.H. Palacios, P.L. Mote, M. Scheibye-Knudsen, et al., Metformin improves healthspan and lifespan in mice, N. Commun. 4 (2013) 2192.

[33] P. Naik, N. Fofaria, S. Prasad, R.K. Sajja, B. Weksler, P.O. Couraud, et al., Oxidative and pro-inflammatory impact of regular and denicotinized cigarettes on blood brain barrier endothelial cells: is smoking reduced or nicotine-free products really safe?, BMC Neurosci. 15 (2014) 51.

[34] S. Prasad, R.K. Sajja, J.H. Park, P. Naik, M.A. Kaisar, L. Cucullo, Impact of cigarette smoke extract and hyperglycemic conditions on blood-brain barrier endothelial cells, Fluids Barriers CNS 12 (2015) 18.

[35] R.K. Sajja, S. Prasad, L. Cucullo, Impact of altered glycaemia on blood-brain barrier endothelium: an in vitro study using the hCMEC/D3 cell line, Fluids Barriers CNS 11 (2014) 8.

[36] R.J. Dowling, S. Niraula, V. Stambolic, P.J. Goodwin, Metformin in cancer: translational challenges, J. Mol. Endocrinol. 48 (2012) R31–R43.

[37] A. Alfieri, S. Srivastava, R.C. Siow, D. Cash, M. Modo, M.R. Duchen, et al., Sulforaphane preconditioning of the Nrf2/HO-1 defense pathway protects the cerebral vasculature against blood-brain barrier disruption and neurological deficits in stroke, Free Radic. Biol. Med. 65 (2013) 1012–1022.

[38] K.M. Holmstrom, R.V. Kostov, A.T. Dinkova-Kostova, The multifaceted role of Nrf2 in mitochondrial function, Curr. Opin. Toxicol. 1 (2016) 80–91.

[39] J.D. Lalau, A.S. Lemaire-Hurtel, C. Lacroix, Establishment of a database of metformin plasma concentrations and erythrocyte levels in normal and emergency situations, Clin. Drug Investig. 31 (2011) 435–438.

[40] X. Liu, R.R. Chhipa, I. Nakano, B. Dasgupta, The AMPK inhibitor compound C is a potent AMPK-independent antiglioma agent, Mol. Cancer Ther. 13 (2014) 596–605.

[41] Y. Mitsuishi, K. Taguchi, Y. Kawatani, T. Shibata, T. Nukiwa, H. Aburatani, et al., Nrf2 redirects glucose and glutamine into anabolic pathways in metabolic reprogramming, Cancer Cell 22 (2012) 66–79.

[42] T. Li, H. Wang, Y. Ding, M. Zhou, X. Zhou, X. Zhang, et al., Genetic elimination

[43] of Nrf2 aggravates secondary complications except for vasospasm after experimental subarachnoid hemorrhage in mice, Brain Res. 1558 (2014) 90–99.

[43] T. Rangasamy, C.Y. Cho, R.K. Thimmulappa, L. Zhen, S.S. Srisuma, T.W. Kensler, et al., Genetic ablation of Nrf2 enhances susceptibility to cigarette smoke-induced emphysema in mice, J. Clin. Investig. 114 (2004) 1248–1259.

[44] D. Goven, A. Boutten, V. Lecon-Malas, J. Marchal-Somme, N. Amara, B. Crestani, et al., Altered Nrf2/Keap1-Bach1 equilibrium in pulmonary emphysema, Thorax 63 (2008) 916–924.

[45] E.H. Heiss, D. Schachner, K. Zimmermann, V.M. Dirsch, Glucose availability is a decisive factor for Nrf2-mediated gene expression, Redox Biol. 1 (2013) 359–365.

[46] L.M. Aleksunes, S.A. Reisman, R.L. Yeager, M.J. Goedken, C.D. Klaassen, Nuclear factor erythroid 2-related factor 2 deletion impairs glucose tolerance and exacerbates hyperglycemia in type 1 diabetic mice, J. Pharmacol. Exp. Ther. 333 (2010) 140–151.

[47] J. Kang, M.G. Jeong, S. Oh, E.J. Jang, H.K. Kim, E.S. Hwang, A FoxO1-dependent, But NRF2-independent induction of heme oxygenase-1 during muscle atrophy, FEBS Lett. 588 (2014) 79–85.

[48] M.S. Piao, J.J. Park, J.Y. Choi, D.H. Lee, S.J. Yun, J.B. Lee, et al., Nrf2-dependent and Nrf2-independent induction of phase 2 detoxifying and antioxidant enzymes during keratinocyte differentiation, Arch. Dermatol. Res. 304 (2012) 387–395.

[49] N.G. Abraham, A. Kappas, Pharmacological and clinical aspects of heme oxygenase, Pharmacol. Rev. 60 (2008) 79–127.

[50] A.W. Bruijnzeel, R.M. Bauzo, V. Munikoti, G.B. Rodrick, H. Yamada, C.A. Fornal, et al., Tobacco smoke diminishes neurogenesis and promotes gliogenesis in the dentate gyrus of adolescent rats, Brain Res. 1413 (2011) 32–42.

[51] L. Wang, K.J. Colodner, M.B. Feany, Protein misfolding and oxidative stress promote glial-mediated neurodegeneration in an Alexander disease model, J. Neurosci. 31 (2011) 2868–2877.

[52] K. Kruger, G. Dischereit, M. Seimetz, J. Wilhelm, N. Weissmann, F.C. Mooren, Time course of cigarette smoke-induced changes of systemic inflammation and muscle structure, Am. J. Physiol. Lung Cell Mol. Physiol. 309 (2015) L119–L128.

[53] R. Pryor, F. Cabreiro, Repurposing metformin: an old drug with new tricks in its binding pockets, Biochem. J. 471 (2015) 307–322.

[54] A. Chiolero, D. Faeh, F. Paccaud, J. Cornuz, Consequences of smoking for body weight, body fat distribution, and insulin resistance, Am. J. Clin. Nutr. 87 (2008) 801–809.

[55] Q. Ma, X. He, Molecular basis of electrophilic and oxidative defense: promises and perils of Nrf2, Pharmacol. Rev. 64 (2012) 1055–1081.

[56] T. Muller, A. Hengstermann, Nrf2: friend and foe in preventing cigarette smoking-dependent lung disease, Chem. Res. Toxicol. 25 (2012) 1805–1824.

[57] Y. Shintani, S. Maruoka, Y. Gon, D. Koyama, A. Yoshida, Y. Kozu, et al., Nuclear factor erythroid 2-related factor 2 (Nrf2) regulates airway epithelial barrier integrity, Allergol. Int. 64 (Suppl.) (2015) S54–S63.

[58] Y. Wei, X. Zhang, L. Xu, S. Yi, Y. Li, X. Fang, et al., The effect of cigarette smoke extract on thrombomodulin-thrombin binding: an atomic force microscopy study, Sci. China Life Sci. 55 (2012) 891–897.

[59] D.G. Hardie, AMP-activated protein kinase: an energy sensor that regulates all aspects of cell function, Genes Dev. 25 (2011) 1895–1908.

[60] B. Viollet, S. Horman, J. Leclerc, L. Lantier, M. Foretz, M. Billaud, et al., AMPK inhibition in health and disease, Crit. Rev. Biochem. Mol. Biol. 45 (2010) 276–295.

[61] J.S. Lee, S.J. Park, Y.S. Cho, J.W. Huh, Y.M. Oh, S.D. Lee, Role of amp-activated protein kinase (AMPK) in smoking-induced lung inflammation and emphysema (Seoul)Tuberc. Respir. Dis. 78 (2015) 8–17.

[62] M.S. Joo, W.D. Kim, K.Y. Lee, J.H. Kim, J.H. Koo, S.G. Kim, AMPK facilitates nuclear accumulation of Nrf2 by Phosphorylating at serine 550, Mol. Cell Biol. 36 (2016) 1931–1942.

[63] C. Mo, L. Wang, J. Zhang, S. Numazawa, H. Tang, X. Tang, et al., The crosstalk between Nrf2 and AMPK signal pathways is important for the anti-inflammatory effect of berberine in LPS-stimulated macrophages and endotoxin-shocked mice, Antioxid. Redox Signal 20 (2014) 574–588.

[64] K. Zimmermann, J. Baldinger, B. Mayerhofer, A.G. Atanasov, V.M. Dirsch, E.H. Heiss, Activated AMPK boosts the Nrf2/HO-1 signaling axis—A role for the unfolded protein response, Free Radic. Biol. Med. 88 (2015) 417–426.